Emission spectroscopy of photodissociating N_2O_4 excited near 200 nm to the $\pi_{nb,O}\pi^*_{NO_2}/n\sigma^*_{N-N}$ avoided crossing

B. F. Parsons, S. L. Curry, J. A. Mueller, P. C. Ray, and L. J. Butler[a)]
The James Franck Institute and Department of Chemistry, The University of Chicago, Chicago, Illinois 60637

(Received 6 July 1999; accepted 18 August 1999)

These experiments and complementary electronic structure calculations seek to probe the early dissociation dynamics of N_2O_4 excited in the strong 186 nm ultraviolet absorption band. Laser photons of 199.7, 203, and 205 nm are used to dissociate N_2O_4 molecules expanded in a free jet. The emission from the dissociating molecules is dispersed in a spectrometer and collected with an optical multichannel analyzer (OMA). We observe a strong progression in ν_3, the N–N stretching mode, consistent with electronic structure calculations and a previous observation of N–N bond fission leading to NO_2 photoproducts in this band. We also observe emission to combination bands in ν_4, the torsion, and ν_5, the out-of-phase antisymmetric NO_2 stretch, which we attribute to vibronic coupling to a $\sigma\sigma^*$ excited state configuration. Analysis of our data allows for an assignment of the torsional frequency of N_2O_4. Around 200 nm nitric acid, nitromethane, and N_2O_4 all exhibit a similar absorption to an adiabatic surface that changes electronic character from $\pi_{nb,O}\pi^*_{NO_2}$ at short O_2N–R (R=CH_3, OH, NO_2) internuclear distances to $n\sigma^*$ at extended internuclear distances. We compare our present emission spectra of N_2O_4 with previous emission experiments on nitromethane to understand how the character of the Franck–Condon region of the excited states in these two molecules differ. © *1999 American Institute of Physics.* [S0021-9606(99)01442-7]

I. INTRODUCTION

Molecules with NO_2 functional groups and molecules well described as covalently bonded clusters[1] play a key role in atmospheric chemistry, yet much of their photochemistry and photophysics is still poorly understood. In this work we seek to compare and contrast the early photofragmentation dynamics of the NO_2 dimer, N_2O_4, upon excitation in the strong 186 nm ultraviolet absorption band with those of nitric acid and nitromethane excited in the analogous $\pi_{nb,O}\pi^*_{NO_2}$ absorption band[2] characteristic of molecules with NO_2 functional groups. Of particular interest in this study are (1) how torsional motion and antisymmetric stretching are coupled in the early dissociation dynamics and (2) how Franck–Condon access to the excited electronic state from a ground state with an unusually long equilibrium N–N bond length could probe the region of avoided crossing of the $\pi_{nb,O}\pi^*_{NO_2}$, and $n\sigma^*$ electronic configurations along the N–N bond fission excited-state reaction coordinate.

The structure of N_2O_4 has been studied by x-ray diffraction,[3–5] neutron diffraction in the crystal,[6] and gas-phase electron diffraction.[7–9] The lowest-energy structure of this molecule has D_{2h} symmetry with an exceptionally long NN bond, 1.75–1.782 Å. Additionally, the NO bond, 1.190 Å, and the ONO bond angle, 135.4°, are little changed from the values in ground state NO_2, 1.199 Å and 133.7°, respectively.[9] Theoretical studies have attempted to explain the unusual features of N_2O_4: the long N–N bond and the planar conformation.[7,10–15] The calculation of an accurate value for the N–N bond length has proven difficult; only recently, by considering the effect of electron correlation, have theoretical bond lengths become consistent with the experiment.[15–20]

Before discussing the electronic character of N_2O_4 excited in the 186 nm absorption band and the interpretation of the few experiments probing the resulting dissociation dynamics, we note that the symmetry labels of the relevant molecular orbitals and the symmetry label given to the excited state accessed depend on the coordinate system chosen for the N_2O_4 molecule. Unfortunately, no single convention for the choice of coordinate axes has been uniformly adopted, and this had led to considerable confusion when experimentalists studying the photofragmentation channels[21,22] have compared their results to the only available excited state electronic structure calculations, those of Mason.[23] The top frame in Fig. 1 depicts the convention for coordinate axes most commonly used by experimentalists[21,22] and most electronic structure theorists,[13–15,24] with the planar molecule in the *XZ* plane and the *Z* axis directed along the N–N bond. The next frame down in Fig. 1 shows the coordinate system adopted in the calculations of the excited states of N_2O_4 by Mason,[23] with the molecule in the *XZ* plane but the *X* axis directed along the N–N bond. Thus, the symmetry of the excited state accessed at 186 nm is given as $1\,^1B_{1u}$ in the work of Mason (with a transition dipole oriented in her *Z* axis direction, in the molecular plane but perpendicular to the N–N bond), but when that label is transformed into the coordinate system used by other elec-

a)Electronic mail: 1-butler@uchicago.edu

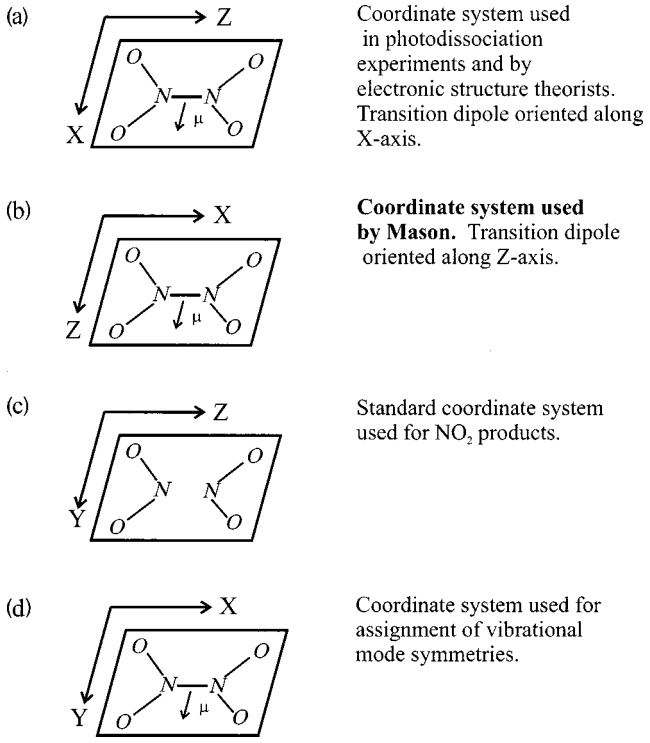

FIG. 1. Common coordinate systems in use for N_2O_4. We use (a) the coordinate system used in electronic spectroscopy throughout for N_2O_4, and (c) for NO_2.

tronic structure theorists and experimentalists it should be redesignated as the $1\,^1B_{3u}$ state. Neither Kawaski and co-workers[21] nor Johnston and co-workers[25] noticed that Mason was using a different coordinate system than they, so the interpretation of their experimental results with respect to Mason's work is in error. In this paper, we adopt the most common coordinate system (Fig. 1, top) used for the electronic configuration of N_2O_4, with the molecule in the *XZ* plane and the *Z* axis along the N–N bond, and where necessary transform the work of Mason to this coordinate system. We also use the nearly universally adopted coordinate system for the NO_2 product, with the molecule in the *YZ* plane and the *Z* axis along the C_2 axis [Fig. 1(c)].

The electronic configuration of N_2O_4 in the ground state (with the coordinate system as depicted in the top of Fig. 1) is[24]

$$\ldots(4b_{3u})^2(4b_{2g})^2(1b_{1g})^2(1a_u)^2(6a_g)^2(2b_{2u})^0(6b_{1u})^0 \times(2b_{3g})^0,$$

where we also show the lowest unoccupied orbitals in the energetic order determined by von Niessen *et al.*[24] The absorption spectrum of N_2O_4 has been previously studied between 240 and 500 nm[26] and between 185 and 390 nm.[27] The spectrum of Bass *et al.*[27] shows a strong broad absorption, indicative of a dissociative transition, peaking between 185 and 190 nm and extending to 230 nm. CNDO/S electronic structure calculations of Mason[23] suggest that the excited state reached is of $1\,^1B_{3u}$ symmetry [Mason's $1\,^1B_{1u}$ label is for a nonstandard coordinate system, Fig. 1(b)] and is best described as a configuration-interaction mixture of two dominant electronic configurations, one in which an electron is promoted from the π nonbonding oxygen molecular orbital to the π^* orbital (a delocalized version of the transition resulting in the strong 190 nm absorption in nitromethane and nitric acid) and the other contributing configuration corresponding to promotion of an electron from a nonbonding in-plane molecular orbital localized on the O atoms to an orbital that has σ^* character with respect to the N–N bond. Thus, in the most commonly used coordinate system, the $1\,^1B_{3u}$ excited state (Mason's $1\,^1B_{1u}$) accessed in the 186 nm absorption band is an admixture of two electronic configurations in the Franck–Condon region,

$$\ldots(4b_{3u})^2(4b_{2g})^1(1b_{1g})^1(1a_u)^2(6a_g)^2(2b_{2u})^1(6b_{1u})^0 \times(2b_{3g})^0,$$

the $\pi_{\mathrm{nb,O}}(1b_{1g})\rightarrow\pi^*(2b_{2u})$ configuration,

and

$$\ldots(4b_{3u})^2(4b_{2g})^1(1b_{1g})^2(1a_u)^2(6a_g)^2(2b_{2u})^0 \times(6b_{1u})^1(2b_{3g})^0,$$

the $n_{\mathrm{O}}(4b_{2g})\rightarrow\sigma^*(6b_{1u})$ configuration,

with the transition moment directed perpendicular to the N–N axis and in the molecular plane. [Kawasaki *et al.*[21] and Sisk *et al.*[22] mistakenly described Mason's assignment as $\sigma(6a_g)\rightarrow\sigma^*(6b_{1u})$ because they did not realize that Mason was using a different coordinate system than most other workers.]

The photodissociation of N_2O_4 has been investigated previously in both the 186 nm absorption band[21,22] and in the lower-energy absorption bands.[28,29] There is evidence for a competition between N–N fission and N–O fission upon excitation at 280 and 265 nm in the lower absorption bands.[25,28,29] We review only the photofragmentation results upon excitation in the 186 nm absorption band since they are most relevant to our emission spectroscopy studies, performed at excitation wavelengths near 200 nm.

Kawasaki *et al.*[21] observed the time-of-flight spectrum of photofragments from N_2O_4 dissociated at 193 and 248 nm. They detected the signal from neutral photofragments, which gave NO_2^+ upon electron bombardment ionization, but were not able to observe a signal at NO^+ or O^+. This limitation prevented them from probing a potential N_2O_3+O product channel. Slow photofragments were obscured by a laser-independent but time-dependent background, presumably from the pulsed beam source. Four direct dissociation channels were considered in these studies:

$$N_2O_4+h\nu\rightarrow NO_2+NO_2, \quad (1)$$

$$N_2O_4\rightarrow N_2O_3+O, \quad (2)$$

$$N_2O_4\rightarrow NO_3+NO, \quad (3)$$

$$N_2O_4\rightarrow NO_2+NO+O. \quad (4)$$

Based on the available energy after dissociation and the observed translational energy distributions of the photofragments, only (1) and (3) could result in the fastest observed signal at NO_2^+ at either 193 or 248 nm. Since no NO^+ was

detected, Kawasaki *et al.*[21] concluded that (1) is the primary channel at both wavelengths. (This is a problematic argument because a vibrationally or electronically excited NO_2 product is known[30–32] to also produce NO^+ daughter ions, and because energetic considerations only precluded the other channels for the fastest products. One cannot conclude that some of the slower signals at NO_2^+ do not result from the other channels; the lack of data at any other ion precludes any further analysis.) Kawasaki *et al.* note that the maximum energy released to product translation at 193 nm is consistent with the formation of NO_2 molecules in either the $\tilde{A}\ ^2B_2$ or $\tilde{B}\ ^2B_1$ states. However, based on fluorescence measurements they believe the $\tilde{B}\ ^2B_1$ is largely formed from the photolysis at 193 nm. Finally, the 193 nm photodissociation resulted in a parallel photofragment angular distribution, $\beta=1.2$. This is particularly surprising since the electronic structure calculation of Mason[23] indicated the absorption at 193 nm is carried by a transition moment perpendicular to the N–N bond, similar to that for nitromethane[33] and nitric acid,[31,32] but Kawasaki's paper misses the discrepancy because of the confusion over the symmetry label of the excited state in the different coordinate systems used by the two groups.

Sisk *et al.*[22] later studied the fluorescence of NO_2^* from the photodissociation of N_2O_4 at 193, 248, and 351 nm. By coanalyzing their photolysis-induced fluorescence data with the time-of-flight data of Kawasaki *et al.*, they determine that photolysis at 193 nm leads to two NO_2^* fragments in the $\tilde{A}\ ^2B_2$ state. [They note that the assignment of the product channel is more uncertain than at 351 nm, where they assign the product channel to be $NO_2(\tilde{X}\ ^2A_1)+NO_2^*(\tilde{B}\ ^2B_1)$, where the $NO_2(\tilde{B}\ ^2B_1)$ is vibrationally excited.] Sisk *et al.*[22] mistakenly refer to the 186 nm electronic transition calculated by Mason as $\sigma(6a_g)\rightarrow\sigma^*(6b_{1u})$, missing the change in the coordinate system described above, so their subsequent discussion of a possible electronic curve crossing in the dynamics is in error.

In this paper we report the dispersed emission from photodissociating N_2O_4 excited at several wavelengths near 200 nm. The emission spectra evidence activity in the N–N stretch and in progressions in antisymmetric stretching modes in combination with torsion. The spectra presented here allow us to correct the literature value of the ground state torsional mode frequency and, when combined with other workers' results, give a gas phase frequency for ν_6, the out-of-phase NO_2 rocking mode. We also report complementary CIS *ab initio* electronic structure calculations of some of the relevant excited states of N_2O_4. In the discussion we attempt to elucidate the origin of the early part of the dissociation dynamics revealed in the emission spectra and we speculate how it may influence the branching to different final product channels.

II. EXPERIMENT

The instrumentation used in these experiments has been discussed previously,[34,35] so we give only a brief description here. The laser light used was generated either by anti-Stokes Raman shifting 266 nm light in H_2 or by tripling the output of a Nd:YAG-pumped dye laser. The 532 nm output of a Quantel YG580-C series Nd:YAG laser operating at 20 Hz pumps a Lambda Physik FL3002E dye laser with an intracavity etalon to reduce the bandwidth of the dye laser to 0.05 cm^{-1}. Rhodamine 640 dye was used to generate light between 609 and 615 nm. The output of the dye laser was frequency doubled in a KDP crystal (Lambda Physik FL 30), giving between 7 and 9 mJ per pulse. The 300 and 600 nm beams were frequency summed in a BBO crystal (Inrad 561-044). A Pellin–Broca prism then separated the colinear 200, 300, and 600 nm photons.

The 199.7 nm light was generated by Raman shifting the 266 nm output of an injection-seeded Nd:YAG laser (Continuum PowerLight 9020) in H_2. A 50 cm focal length plano-convex lens was used to focus the ~200 mJ/pulse 266 nm light into the Raman cell. This cell, a 70 cm long stainless steel tube fitted with 3/8 in. thick Suprasil windows at either end, is filled with H_2 to pressure of 50 psig. The divergent output of the Raman cell contained colinear Stokes and anti-Stokes shifted light as well as the 266 nm fundamental; this light was recollimated with a 16 in. focal length plano-convex lens whose position was optimized for the 199.7 or 218 nm light. The light to be used in the experiments was separated from the other wavelengths using a Pellin–Broca prism and finally focused with a 16 in. focal length lens so the light would overlap well with the free jet expansion.

The NO_2/N_2O_4 was introduced into the vacuum chamber as a free jet expansion from an IOTA ONE pulsed valve (General Valve Corp) with an open time of 200–260 μs for each gas pulse. The excitation light interacted with the free jet expansion about 1.0 cm from the pulsed nozzle orifice. Neat NO_2 (Matheson 99.5%) was used for most experiments, but some were performed with 10 % NO_2 in He (Matheson) to confirm that the observed spectra were from N_2O_4 and not higher-order clusters. The backing pressure of the gas was varied between 150 and 800 Torr to control the amount of NO_2 in the expansion and provide further evidence against emission from this species.

Light scattered at 90° to the incident laser propagation direction was collected with a 4 inch focal length lens and focused with a 10 inch focal length lens onto the entrance slit of a spectrometer (Acton SpectraPro 275), which dispersed the light using a 2400 gr/mm holographic grating (Milton-Roy). The dispersed light was then imaged onto an optical multichannel analyzer, OMA, (EG&G PARC 1456B-990-HQ) equipped with a blue-enhanced intensifier and 990 active pixels. Spectral resolution is limited by the spectrometer length and grating and is about 25 cm^{-1}, using a 2400 gr/mm grating. The linear dispersion in the spectra here were calibrated using the laser line and the known Hg line at 230.2065 nm.

III. THEORETICAL METHOD

Ab initio electronic structure calculations were performed using the GAUSSIAN 94[36] program package to characterize the excited state accessed in the experiments and help understand the emission spectra. The vertical excited-state calculations were based on ground state equilibrium geometries obtained from gas phase electron diffraction studies.[8] A configuration interaction with single excitation (CIS) cal-

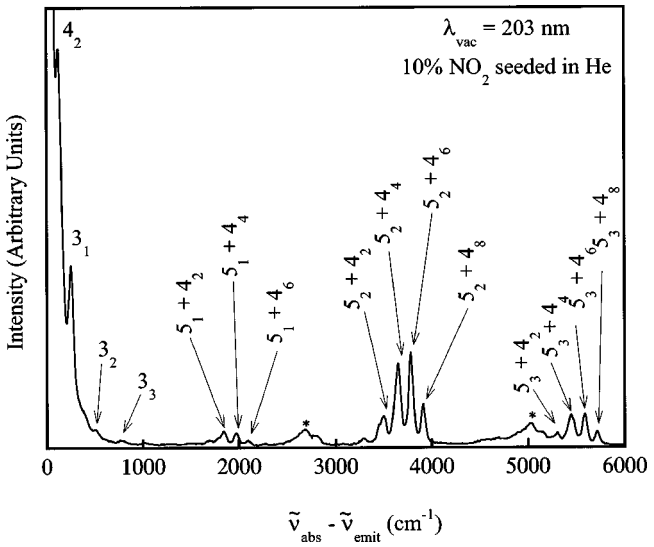

FIG. 2. Emission spectrum of N_2O_4 formed in a 10% NO_2 in He expansion with excitation at 203 nm. Peaks are labeled as the final vibrational eigenstates, assuming the molecule was in the lowest vibrational eigenstate before excitation (for hot bands the assignment corresponds to the change in vibrational quanta in the final state). Labels are $3_n:n$ vibrational quanta in the N–N stretch normal mode, ν_3; $4_n:n$ vibrational quanta in the torsional normal mode, ν_4; $5_n:n$ vibrational quanta in the out-of-phase antisymmetric stretch normal mode, ν_5. Starred features are fluorescence from the NO γ band (see the discussion in Sec. IV E). The features in this spectrum are due to N_2O_4 (see the discussion in Sec. IV A).

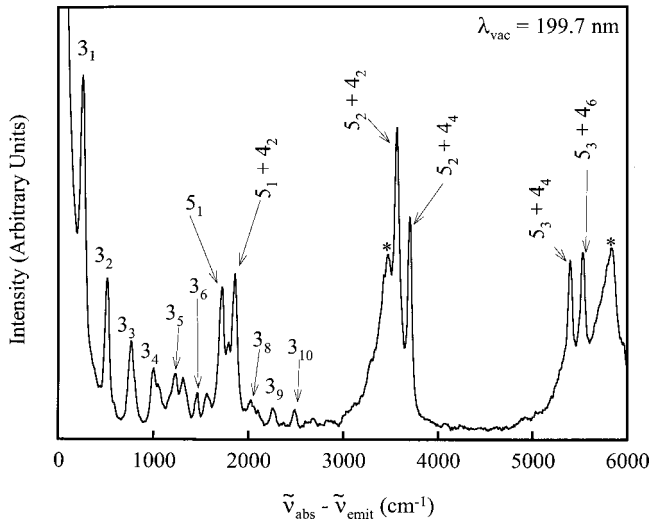

FIG. 3. Emission spectrum of N_2O_4 formed in a neat NO_2 expansion with excitation at 199.7 nm. Labels are the same as in Fig. 2.

culations using a 6-311+G(d,p) basis set generated the oscillator strengths, orbital symmetries, and vertical excitation energies presented here. Symmetry and bonding character of the orbitals contributing to the excitation were classified using the linear combinations of atomic orbitals output by the Gaussian program.

Potential energy curves depicted in the paper were generated by repeating the vertical excitation calculation at incremental bond separations or angles. At each geometry, the program computes the ground state energy at the MP2 level of theory.

IV. RESULTS

A. Eliminating the contribution of NO_2 and higher order clusters of N_2O_4

The absorption cross section of NO_2 is about two orders of magnitude smaller than that of N_2O_4 around 200 nm.[22] Thus, we expect the contribution of NO_2 to our emission spectra to be much less than the contribution from N_2O_4. Furthermore, the features in the emission spectra collected in this wavelength region are very easily assigned to either individual N_2O_4 normal modes or combinations of them, while an assignment to the modes of NO_2 proved impossible. We checked for the contribution of higher-order $(NO_2)_n (n \geq 3)$ clusters in the observed emission spectra by minimizing the number of higher-order clusters in the expansion. Sisk *et al.* observed that higher-order clusters could be minimized by using 10% NO_2 seeded in He.[22] Figure 2 presents the emission spectrum at 203 nm using 10% NO_2 in He, and Fig. 4 shows the emission spectrum at 203 nm using neat NO_2. The qualitative features of these two spectra are the same. Both spectra show a progression assigned as the N–N stretch and a series of combination bands involving the out-of-phase antisymmetric stretch and torsion (assignments will be discussed in the following section). Thus, the identical features in the 203 nm spectrum taken using neat NO_2 are due to N_2O_4. Hence, all later spectra were collected using neat NO_2, which we found to give a better signal-to-noise ratio.

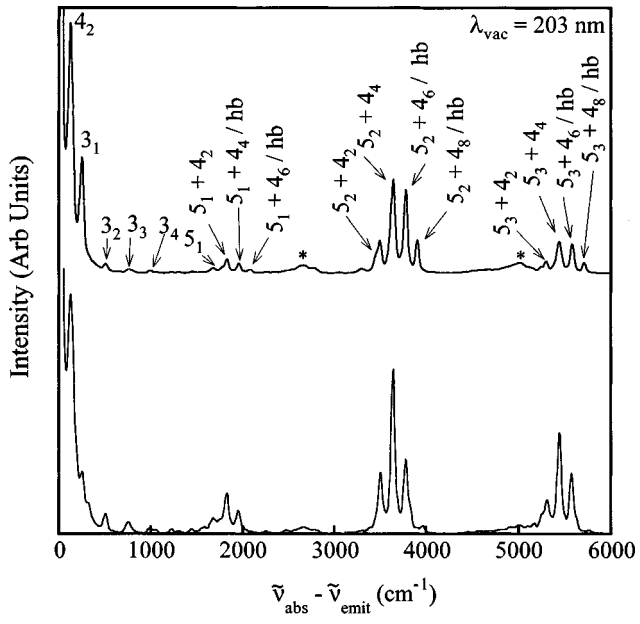

FIG. 4. Emission spectrum of N_2O_4 formed in a neat NO_2 expansion with excitation at 203 nm. The top spectrum was taken with 600 Torr backing pressure. Labels are as in Fig. 2. The similarity of this spectrum to that in Fig. 2 indicates that the features are due to N_2O_4. The bottom spectrum was taken with 750 Torr backing pressure. The reduction in intensity of the $\nu_5 + \nu_4$ combination bands with highest torsional motion indicates these result from molecules with a thermal population in higher torsional levels of the ground electronic state (see the discussion in Sec. IV B).

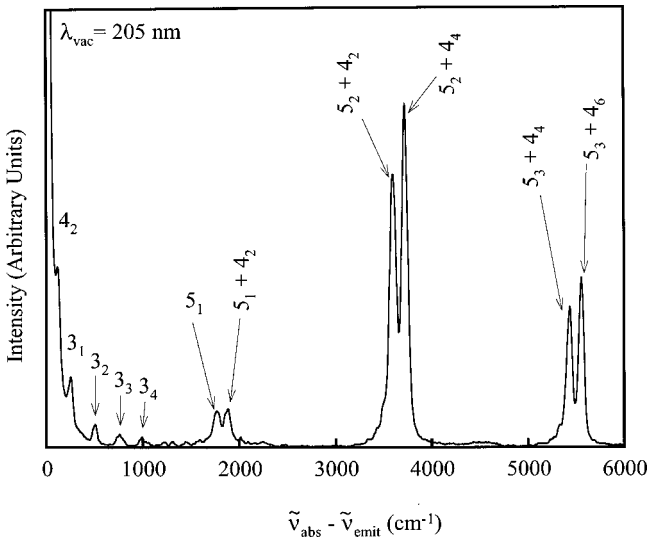

FIG. 5. Emission spectrum of N_2O_4 formed in a neat NO_2 expansion with excitation at 205 nm. Labels are as in Fig. 2.

B. Emission features at 199.7, 203, and 205 nm

The emission spectra of N_2O_4 collected with laser excitation at 199.7, 203, and 205 nm are presented in Figs. 3–5, respectively. The emission spectra of N_2O_4 all share several interesting features. All of the spectra show a progression with the first peak near 260 cm^{-1} and the spacing between subsequent peaks of about 255 cm^{-1}. Since Dyer and Hendra assigned the frequency of ν_3, the N–N stretch, as 254 cm^{-1},[37] this progression is easily assigned as a progression in ν_3, the N–N stretch. The 199.7 nm spectrum shows a long progression in the N–N stretching motion, with resolved peaks extending to ten quanta in ν_3. The 3_7 (when referring to the change in the number of vibrational quanta in a given normal mode, we use this notation throughout, where 3_7 refers to an additional seven vibrational quanta in ν_3 after photon absorption and emission) peak comes at slightly larger shifts than the fundamental of ν_5, the out-of-phase antisymmetric stretch, and is not labeled in the spectrum.

A second progression appears in these spectra, starting at about 1725 cm^{-1}. The vibrational frequency of ν_5, the out-of-phase antisymmetric stretch, is 1712 cm^{-1}.[38] The only other mode near 1725 cm^{-1} is the in-phase antisymmetric stretch, ν_9, which occurs around 1735 cm^{-1} but it is disallowed by selection rules.[38] Thus, the fundamental peak in this progression is assigned as ν_5. We discuss how emission into odd quanta of ν_5 may be vibronically allowed later in this section.

The next peaks in this progression are spaced by a frequency of about 135 cm^{-1}. This corresponds closely to our value for $2\nu_4$ (see the discussion in Sec. IV D). The next peak is thus assigned as 5_1+4_2. The peak near 3570 cm^{-1} is assigned as 5_2+4_2. Assuming the torsional frequency increases with excitation of ν_5 (which we observe in the case of 5_1+4_2), then this value is about 15 cm^{-1} lower than expected. The next peak is again about 135 cm^{-1} away and is assigned as 5_2+4_4. The final peaks in the spectrum appear at 5400 and 5530 cm^{-1} and are assigned as 5_3+4_4 and 5_3+4_6, respectively.

Figure 4 presents the emission spectra taken at 203 nm under two different expansion conditions. The peaks are assigned similarly to those in the 199.7 nm. The spectra again show a progression in the N–N stretch, ν_3. Again, out-of-phase antisymmetric stretch and the torsion are present in combination bands. In the top spectrum in Fig. 4, the combination bands appear as a series of ''quartets.'' We note that the spacing decreases between the peaks in the series 5_1, 5_1+4_2, 5_1+4_4, and 5_1+4_6. This is likely due to the anharmonicity of the oscillator though the resolution of the detector limits this analysis. We repeated the 203 nm spectrum using neat NO_2 at higher backing pressures around 750–800 Torr, shown in Fig. 4, bottom spectrum. The combination bands of ν_5 and ν_4 in this spectrum (Fig. 4 bottom) appeared as a series of ''triplets'' corresponding to the first three peaks from the ''quartets'' in Fig. 4 (top) spectrum. The final peak in the combination bands is evident, though much reduced in intensity. The increase in backing pressure should favor additional cooling of molecular rotation, and to a lesser extent, vibrations. The changes in the spectra under these different experimental conditions may result from a decrease in the contribution of hot bands to the spectrum taken at the higher backing pressure. If a low-energy motion such as ν_4 is present in the molecule, then a significant vibrationally excited population exists at 298 K. Thus, if a molecule in the 4_1 vibrational state is excited with a photon and shows emission intensity in the band labeled 5_2+4_6, then the actual vibrational state of the molecule after emission is 5_2+4_7. We explicitly indicate bands with a contribution from hot bands in our 203 nm spectrum with the notation 5_n+4_m/hb, but we do not indicate these in the other figures in the paper.

It is interesting to consider how we can see emission into bands with odd quanta in ν_5. To understand the origin of emission intensity into odd quanta in an antisymmetric mode, nominally an electric–dipole forbidden in emission spectroscopy, we consider the emission in a time-independent formalism in which the intensity is proportional to the square of $\alpha_{fi}(\omega_I)$,

$$\alpha_{fi}(\omega_I)=\sum_n \frac{\langle f|\mu_{\mathrm{em}}\cdot e_S|n\rangle\langle n|\mu_{ab}\cdot e_I|i\rangle}{E_I+\hbar\omega_I-E_n-i\hbar\Gamma}. \tag{5}$$

The subscript *I* stands for incident and *S* stands for scattered, and Γ is a lifetime factor. We consider only the second term, responsible for emission, making the assumption that all molecules emit from the same excited electronic state. The intermediate state, $|n\rangle$, and the final state, $\langle f|$, can be expressed as a product of rotational, vibrational, and electronic states. Assuming that the rotational part can be factored out (neglecting Coriolis coupling) the intermediate and final states become

$$|n\rangle=|(\nu e)_n\rangle, \tag{6}$$

$$\langle f|=\langle(\nu e)_f|. \tag{7}$$

Finally, we assume that the initial $1\,{}^1B_{3u}\leftarrow\tilde{X}\,{}^1A_g$ excitation is from the a_g ground vibrational level in the ground electronic state, so the operative transition moment μ_{ab} is b_{3u} [as in Fig. 1(a)] and the intermediate, $|n\rangle$, vibrational symmetry

is then a_g. Then emission to a b_{2g} vibrational state (ν_5) of an A_g electronic state from an a_g vibrational level of the B_{3u} state requires a dipole moment to have the symmetry of the product $b_{2g}\otimes A_g\otimes a_g\otimes B_{3u}=b_{1u}$[39] (note that we are assuming the electronic coordinate system [Fig. 1(a)] and use the vibrational symmetry of ν_5 in this coordinate system). Thus, the term for emission becomes

$$\langle b_{2g}A_g|b_{1u}|a_gB_{3u}\rangle. \tag{8}$$

According to Table II, the ninth excited state has B_{1u} symmetry and a very large oscillator strength. This state seems a likely candidate for the intensity borrowing[40] required for vibronically allowed emission into these antisymmetric vibrational modes.

Finally, we investigated the dependence of the emission intensity on the polarization of the 203 nm excitation laser. This technique has proven useful in the identification of emission features resulting from a state with a transition dipole oriented perpendicular to that for absorption.[33,41] Using 600 Torr of neat NO_2 (conditions known to give ''quartets'' in the antisymmetric stretch/torsion progression), we found that the second peak in each quartet (assigned as $5_n+4_{2n}; n=1,2,3$) was reduced in intensity when the incident laser light was polarized parallel to the plane defined by the detector and the direction of propagation of the laser beam. These peaks in the quartets must then result from two different transitions from the excited state, one with a transition dipole oriented perpendicular to that for absorption and one oriented the same as for absorption. However, we have been unable to find another assignment of these peaks. Emission by a vibronic mechanism requires the polarization of the emitted photon to be directed along the N–N bond [since b_{1u} transforms as the Z axis in the electronic coordinate system; Fig. 1(a)]. Thus, the intensity of the combination bands should depend upon the polarization studied. However, if the emission occurs slowly (on the time scale of molecular rotations) then the intensity dependence on polarization will be reduced.

Figure 5 shows the emission spectrum of N_2O_4 excited at 205 nm. Again, we observe a feature in this spectrum at *ca.* 255 cm^{-1} assigned as 3_1. A progression in ν_3, the N–N stretch, appears with a spacing of 255 cm^{-1} and extends to four quanta. A progression in combination bands of the out-of-phase antisymmetric stretch with even quanta of torsion also appears. The combination bands appear as a series of ''doublets'' spaced by about 140 cm^{-1} or 4_2 (the peaks are assigned as discussed and not discussed in detail here). Finally, a relatively weak line appears at 128 cm^{-1}, which we again assign as the torsion.

C. Gas phase assignments for the torsional frequency, ν_4, and out-of-phase NO_2 rock, ν_6

The first feature in the 203 nm spectrum is shifted from the laser line by 128 cm^{-1}. The only vibration with a frequency under 250 cm^{-1} is the torsion,[38] and while a single quantum in the torsional mode is symmetry disallowed for both Raman and IR spectroscopy, even quanta of any motion are symmetry allowed. The only other possibility is that this peak is due to an impurity with a vibrational frequency near 64 cm^{-1}, in addition to a mode around 1725 cm^{-1} (since we observe a mode near 130 cm^{-1} coupled with a motion near 1700 cm^{-1}). The molecule O_2NNO has a torsional frequency at 63 cm^{-1} but does not have a mode around 1725 cm^{-1}.[38] The antisymmetric NO dimer, ONON, has vibrational frequencies of 116 and 1690 cm^{-1}.[42] However, this molecule was observed in the presence of strong Lewis bases at 77 K and is unlikely to occur in our free jet. Thus, we assign this feature as 4_2. This is the first observation of the torsional motion in N_2O_4 not in combination with any other band; the previous assignment of the ground state torsional frequency was obtained from a combination band with ν_6.[43,44] Both groups observed combination bands assigned as $(\nu_6+\nu_4')+n'\nu_4'-n''\nu_4''$ (ν_6 is the out-of-phase NO_2 rock, ν_4' is the torsional frequency with the ν_6 vibration singly excited, and ν_4'' refers to the torsional frequency with ν_6 in the ground vibrational state). The vibrational frequencies were then fit to potentials modeling the torsion with ν_6 in its ground and first excited state. Both groups assumed the value of ν_6 to be 480 cm^{-1} (a value taken from a combination of liquid and vapor phase data).[43,44] However, with our more direct observation of ν_4, the value of the torsional frequency should be revised to 64 cm^{-1}. Using our value of the torsional frequency and the frequencies of the first two peaks in the work of Bibart and Ewing,[43] we can derive a value for ν_6. The difference between the value for $\nu_6+\nu_4'=554.3\,cm^{-1}$ and $(\nu_6+\nu_4')+\nu_4'-\nu_4''=547.7\,cm^{-1}$ gives $\nu_4'-\nu_4''=-6.6\,cm^{-1}$. Combining our value for the ground state torsional frequency with the difference $\nu_4'-\nu_4''=-6.6\,cm^{-1}$ gives a value for the torsional frequency with ν_6 singly excited of about 57 cm^{-1}. Combining this result with $\nu_6+\nu_4'=554.3\,cm^{-1}$ gives a gas phase value of ν_6 as 497 cm^{-1}, in close agreement with the value obtained using Ne matrices.[45]

TABLE I. Fluorescence energy of NO.

v'-v''	Literature NO band heads[a]	$\tilde{\nu}_{abs}$ (cm^{-1})	$\tilde{\nu}_{abs}$-$\tilde{\nu}_{emit}$ (cm^{-1})	Emitted photon energy[b] $\tilde{\nu}_{emit}$ (cm^{-1})
0–0	44 197.48	50 075	5835	44 240
0–0	44 197.48	49 247	5020	44 227
1–0	46 539.36	50 075	3430	46 645
1–0	46 539.36	49 247	2665	46 582

[a]Values are for the Q_{11} from J. Danielak, U. Domin, R. Kepa, M. Rytel, and M. Zachwieja, J. Mol. Spectrosc **181**, 394 (1997).
[b]Determined from our spectra.

D. Assignment of NO fluorescence

The spectra taken at 199.7, 203, and 205 nm all exhibit two broad peaks that we attribute to NO ($\tilde{A}$) fluorescence. The wave number, $\tilde{\nu}_{abs}$, of the excitation energy and position of the maximum, $\tilde{\nu}_{abs}-\tilde{\nu}_{emit}$, for these peaks in the spectra are given in Table I. Table I also presents the $Q_{11}(0-0)$ and $(1-0)$ band head positions for fluorescence of NO from the γ band, ($\tilde{A}\,^2\Sigma^+-\tilde{X}\,^2\Pi$).[46] The energy of the maximum for the two broad features corresponds quite well with the energy of the band heads. Thus, we assign the feature around 44 230 cm^{-1} in these spectra to the $(0-0)$ transition of the γ band of NO and the feature around 46 600 cm^{-1} to the

TABLE II. Vertical excitation energies for N_2O_4.

Excited state	Electronic character	Excitation energy (eV)	Oscillator strength
$1\,^1B_{2u}$		4.6	0.0
$1\,^1A_u$		5.3	0.0
$1\,^1B_{1g}$		5.7	0.0
$1\,^1B_{3g}$		6.2	0.0
$1\,^1B_{3u}$	$\pi_{\mathrm{nb,o}}\pi^*_{\mathrm{NO_2}}/n\sigma^*_{\mathrm{N-N}}$	6.9	0.1474
$1\,^1B_{2g}$		7.2	0.0
$2\,^1B_{1g}$		7.3	0.0
$2\,^1A_u$		7.6	0.0
$1\,^1B_{1u}$	$\sigma\sigma^*$	8.1	1.0257
$2\,^1B_{3u}$		9.3	0.5149

$(1-0)$ transition of the γ band of NO. Though the peak positions are in fair agreement with the Q_{11} branch of each fluorescence band, our resolution is too low to make a definitive assignment.

The $\tilde{A}$ state of NO from which we see fluorescence may result from secondary photodissociation of the nascent NO_2 product if it absorbs another photon, or by unimolecular dissociation of the NO_2 photofragment to give $NO(\tilde{X}) + O$, with the $NO(\tilde{X})$ then fluorescing after absorption of a second photon. We judge the former to be more likely since the energy of the $NO(\tilde{A})$ fluorescence is roughly independent of excitation energy.

E. Computational results

Table II gives the vertical excitation energy and symmetries for the excited states calculated using the CIS methods. Each state in this calculation, which includes configuration interaction, can contain contributions from one or more electronic configurations of one-electron excitations from the reference configuration (ground state). The CIS expansion for the bright state accessed in the transition near 200 nm $(1\,^1B_{3u})$ is shown in Table II and the relevant orbitals are depicted in Fig. 6, as visualized using the program SPARTAN.[47] Figures 6(a) and 6(c) are the in- and out-of-phase linear combinations of the same orbitals. Figure 6(a) corresponds to the dominant $\pi\pi^*$ configuration in the excitation and contributes a bonding character to the N–N bond. Figure 6(b) shows the orbitals contributing to the $n\sigma^*_{\mathrm{N-N}}$ electronic character of the excited state. This configuration contributes antibonding character to the N–N bond. The symmetry labels are based on the coordinate convention in Fig. 1(a). When the results of Mason[23] are translated to this coordinate convention, they are in qualitative agreement with the orbitals presented here. The calculated vertical energy of the $1\,^1B_{3u} \leftarrow {}^1A_g$ excitation is greater than 6.67 eV (the 186 nm peak in the absorption spectrum); however, CIS can overestimate the excitation energy by as much as 1–2 eV.[48]

In both nitric acid and nitromethane, a broad absorption is present in the neighborhood of 200 nm. This transition has been previously assigned as $\pi_{\mathrm{nb}}\pi^*$, localized on the NO_2 moiety.[2] The 186 nm transition in N_2O_4 is similar in character, although the excitation is delocalized onto both NO_2 groups. However, in N_2O_4 at the ground state equilibrium geometry, the transition shows a considerable $n\sigma^*$ character. When the N–N bond length is contracted to 1.3 Å, nearer the equilibrium bond lengths for nitromethane and nitric acid, the character of the $1\,^1B_{3u}$ state is $\pi_{\mathrm{nb}}\pi^*$, analogous to both nitric acid and nitromethane.

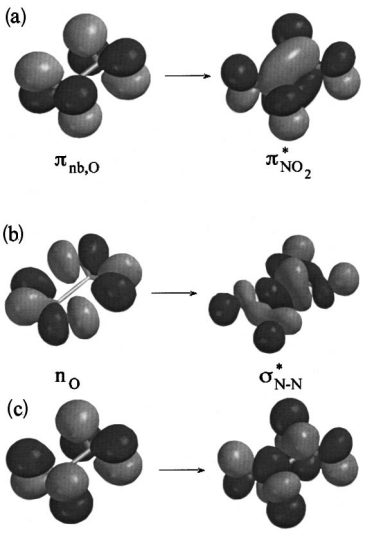

FIG. 6. Orbitals involved in the excitation at 200 nm. (a) Dominant $\pi_{\mathrm{nb,O}}\pi^*_{\mathrm{NO_2}}$ electronic configuration leading to an additional N–N bonding character. (b) $n\sigma^*$ electronic configuration leading to an antibonding N–N character. (c) Minor $\pi_{\mathrm{O}}\pi^*_{\mathrm{NO_2}}$ electronic configuration leading to an antibonding N–N character.

Figure 7 shows a cut along the $1\,^1B_{3u}$ excited state (the state accessed in the 186 nm band) versus N–N bond length. Three higher B_{3u} states, the lowest of which forms an avoided crossing with the $1\,^1B_{3u}$ state, are also depicted in Fig. 7. The avoided crossing at the equilibrium geometry results from a configuration interaction of three one-electron excitations. The dominant one-electron excitations, $\pi_{\mathrm{nb,O}}\pi^*_{\mathrm{NO_2}}$, and $n\sigma^*$, are shown in Figs. 6(a) and 6(b). The

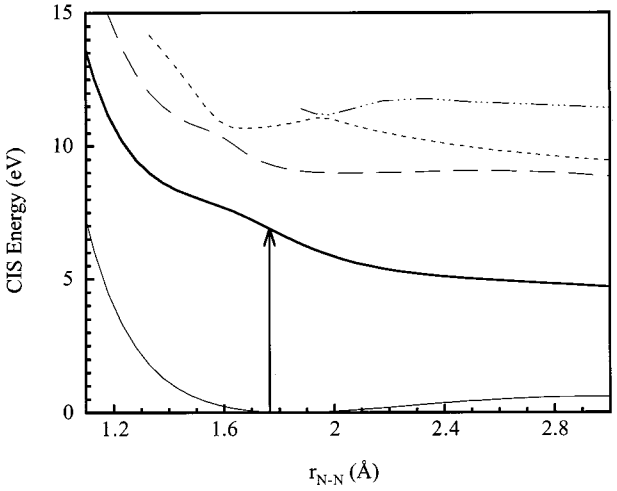

FIG. 7. Excited state potential energy surface for the $^1B_{3u}$ excited states of N_2O_4 vs N–N bond length. The $1\,^1B_{3u}$ is the surface accessed in the transition near 200 nm. The vertical arrow is drawn at the ground state equilibrium geometry to show the Franck–Condon region of the excited state. Note: CIS energies typically overestimate the excitation by 1–2 eV.

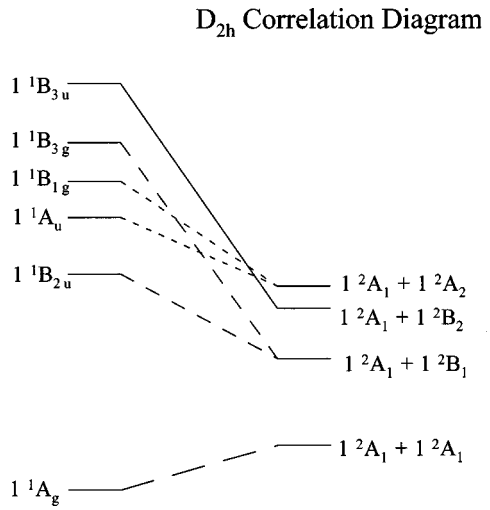

FIG. 8. Adiabatic correlation diagram for N_2O_4 in D_{2h} symmetry dissociating to two NO_2 molecules. N_2O_4 D_{2h} symmetry labels are for N_2O_4 in the *XZ* plane with the *Z* axis along the N–N bond [Fig. 1(a)], the ''standard'' N_2O_4 coordinates, while the NO_2 product symmetry labels are for the fragments in the *YZ* plane [Fig. 1(c)]. The solid line indicates the correlation for the excited state accessed at 200 nm. The relative energies of the NO_2 states are taken using the vertical excitation energies from MRSDCI calculations from Ref. 49 using the ground state NO_2 geometry $\angle ONO = 134°$ and $N–O = 1.193$ Å.

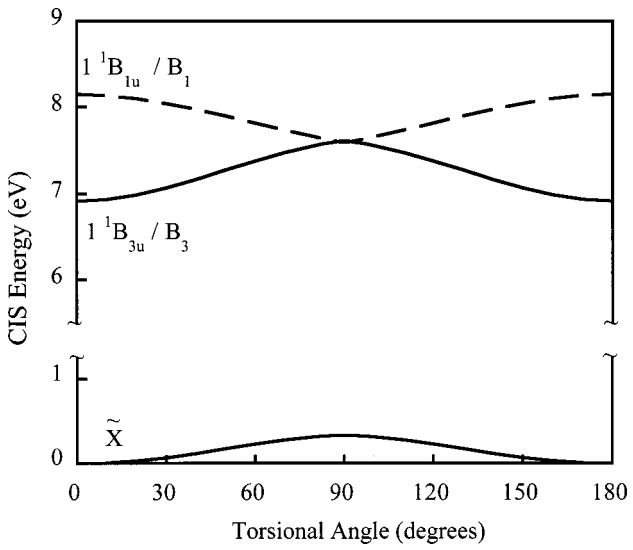

FIG. 10. Potential energy surfaces for the ground state ^1A_g, $1\,^1B_{3u}$, and $1\,^1B_{1u}$ excited states as a function of torsional angle. Bands involving the antisymmetric stretch appear to result from a vibronic interaction between $1\,^1B_{3u}$ and $1\,^1B_{1u}$. The interaction between these two states in nonsymmetric geometries may contribute a force along the torsional coordinate, leading to the observed combination bands of ν_4 and ν_5.

third configuration has a much smaller coefficient in the expansion and is depicted in Fig. 6(c). Figure 8 shows the adiabatic correlation diagram for N_2O_4 in D_{2h} symmetry going to $2NO_2$ and Fig. 9 shows the adiabatic correlation diagram for N_2O_4 in D_2 symmetry going to $2NO_2$. The relative energies of the NO_2 states were determined assuming NO_2 in its ground state equilibrium geometry.[49] Finally, because of the presence of combination bands with multiple quanta in the torsional mode, we calculated the excited state potential as a function of the torsional angle from planar ($\phi = 0°$) through $\phi = 90°$ to planar ($\phi = 180°$). Figure 10 shows a plot of the potential energy as a function of torsional angle holding all other bond lengths and angles fixed at their equilibrium values.

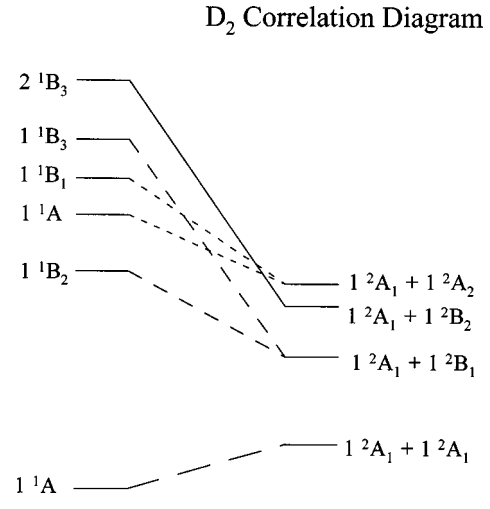

FIG. 9. Adiabatic correlation diagram for N_2O_4 in D_2 symmetry corresponding to the molecular symmetry with the NO_2 groups twisted out of the original plane of the molecule. This corresponds to the lowering of symmetry by torsional motion. The reactant and product molecules are in the same coordinate systems as Fig. 9.

V. DISCUSSION

Emission spectra of N_2O_4 in the region around 200 nm all show a strong progression in ν_3, the N–N bond stretch. The potential energy surface for the $1\,^1B_{3u}$ state accessed in this transition is repulsive along the N–N bond coordinate, as shown in Fig. 7. The CIS calculations indicate that as the N–N bond stretches, only the $1\,^1B_{3u}$ excited state has appreciable oscillator strength (Table II) if one restricts the molecule to D_{2h} symmetry. Thus, the only dynamics yielding a pure progression in the N–N stretch to which we are sensitive are on this state. The explanation of a progression in ν_3 is then simple: when the molecule is initially prepared on the $1\,^1B_{3u}$ adiabat, it feels the repulsive potential and dissociates, giving two NO_2 molecules. A small fraction of the molecules emit light and return to the ground state instead of dissociating, yielding the observed progression.[50,51]

Previous workers[21,22] have observed NO_2 photoproducts tentatively assigned as either the $1\,^2B_2$ or the $1\,^2B_1$ state. As previously discussed, CIS calculations[36] performed at the experimental ground state geometry show the excited state accessed in this transition has B_{3u} symmetry using the standard coordinate convention [Fig. 1(a)]. This transition has two dominant contributions: one from an $n\sigma^*$ electronic configuration and the other from a $\pi\pi^*$ electronic configuration, consistent with the calculations of Mason.[23] The $1\,^1B_{3u}$ potential energy surface correlates adiabatically in D_{2h} symmetry to $NO_2(\tilde{X}\,^2A_1) + NO_2(1\,^2B_2)$ but, as in nitric acid[32] photolysis, the dominant product channel may not be the

adiabatic channel. We are presently pursuing photofragment velocity and angular distribution experiments to determine the dissociation products.

The spectra also evidence strong combination bands involving torsional and antisymmetric stretching. In the results described in Sec. IV B, we noted that emission to bands with odd quanta in ν_5 may be vibronically allowed by coupling to a higher electronic state with B_{1u} symmetry. We noted a likely candidate upon examination of the vertical excitation energies presented in Table II. The $1\,^1B_{1u}$ state, of $\sigma\sigma^*$ electronic character, has a very strong oscillator strength, making it a likely candidate for this vibronic coupling. Furthermore, both the $^1B_{3u}$ and the $^1B_{1u}$ states reduce to B_u symmetry as the molecular framework is displaced along the ν_5 mode, so the lower state may include a small admixture of $\sigma\sigma^*$ character at these geometries. This vibronic coupling with the $1\,^1B_{1u}$ state makes the ν_5 mode active in the emission spectrum. To understand why our emission spectra show ν_5 in combination with the torsional mode, ν_4, we calculated the excited state potential energy surfaces along the torsional angle. The $1\,^1B_{1u}$ state we believe to be involved in the vibronic coupling mechanism has a minimum in the potential energy surface at $\phi = 90°$ (see Fig. 10). Thus, at nonsymmetric geometries the coupling of the $1\,^1B_{1u}$ state with the $1\,^1B_{3u}$ state gives the molecules on the lower state some force along the torsional coordinate, leading to emission into ν_5 in combination with ν_4.

Nitric acid and nitromethane each have an absorption band around 200 nm with $\pi_{\mathrm{nb,O}}\pi^*_{\mathrm{NO_2}}$ electronic character localized on the NO_2 group.[2] Both nitric acid and nitromethane dissociate into $R+NO_2(R=OH, CH_3)$ through two channels; the first forms $NO_2(1\,^2B_2)$ and the second channel has not been definitively assigned.[32,33] The adiabatic surface accessed in both nitric acid and nitromethane changes electronic character from $\pi_{\mathrm{nb,O}}\pi^*_{\mathrm{NO_2}}$ to $n\sigma^*$ at an avoided crossing beyond the Franck–Condon region.[30,32,33] As in N_2O_4 confined to D_{2h} symmetry, the adiabatic surface accessed by nitric acid and nitromethane near 200 nm leads to $NO_2(1\,^2B_2)$. The Franck–Condon region of N_2O_4 has mixed $\pi_{\mathrm{nb,O}}\pi^*_{\mathrm{NO_2}}$ to $n\sigma^*$ electronic character on the bright state. Thus, the emission spectra for N_2O_4 are sensitive to the dynamics at this avoided crossing. Previous studies on the emission spectra of nitromethane obtained at 200 and 218 nm excitation show strong progressions in the NO_2 symmetric stretch and much weaker combination bands of the NO_2 symmetric stretch and C–N stretch.[33,52] The emission spectra collected in solution-phase experiments showed weak features assigned as NO_2 antisymmetric stretch and features due to NO_2 bending motion.[52] The prominence of the progression in the NO_2 symmetric stretch is not surprising because the initial transition is to an electronic state nominally $\pi_{\mathrm{nb,O}}\pi^*_{\mathrm{NO_2}}$ in character.[41,52] Since the final products of the photodissociation are CH_3+NO_2,[30] the excited molecule must eventually reach an electronic configuration repulsive along the C–N bond coordinate. The weak combination bands involving C–N stretch and NO_2 symmetric stretch are possible evidence for this change in electronic character, but in N_2O_4 the pure N–N stretch progression is much stronger, reflecting that N_2O_4 has considerable $n\sigma^*$ character in the Franck–Condon region.

VI. CONCLUSIONS

We reassign the torsional frequency as 64 cm^{-1} and, using the data of previous workers;[43,44] find a value for ν_6 of 497 cm^{-1}, consistent with the value found in Ne matrices.[45] We observe combination bands involving ν_4 and ν_5. The fundamental and second overtone appear to arise from vibronic coupling with a nearby state of $^1B_{1u}$ electronic character.

We have investigated the emission spectroscopy of N_2O_4 at three wavelengths near 200 nm, where the excitation is to the $1\,^1B_{3u}$ surface. Computational results indicate this surface is repulsive along the N–N bond coordinate. Our emission spectra taken near 200 nm all show that the early time dynamics involve a change in the length of the N–N bond, leading to emission into higher overtones of ν_3, the N–N stretch. The adiabatic excited states accessed near 200 nm in N_2O_4, nitric acid, and nitromethane all change from $\pi_{\mathrm{nb,O}}\pi^*_{\mathrm{NO_2}}$ at short O_2N–R ($R=NO_2, OH, CH_3$) bond lengths to $n\sigma^*$ at extended bond lengths. The exceptionally long N–N bond length of N_2O_4 makes the dissociation particularly sensitive to the dynamics near the avoided crossing on the potential energy surface. Thus, the emission spectra of this molecule show strong activity in the N–N stretch normal mode, whereas the emission spectrum of nitromethane near 200 nm shows only weak features involving the C–N stretch. The emission spectrum also shows combination bands in ν_4 and ν_5, tentatively assigned to vibronic coupling with the $1\,^1B_{1u}$ excited state.

ACKNOWLEDGMENTS

This work was supported by the National Science Foundation under Grant No. CHE-9619376. J. Mueller acknowledges support from the Camille and Henry Dreyfus Foundation's Postdoctoral Program in Environmental Chemistry. B. Parsons would like to thank Dr. Fred Arnold for assistance with the SPARTAN program.

[1] V. Vaida, G. J. Frost, L. A. Brown, R. Naaman, and Y. Hurwitz, Ber. Bunsenges. Phys. Chem. **99**, 371 (1995).
[2] L. E. Harris, J. Chem. Phys. **58**, 5615 (1973).
[3] J. S. Broadley and J. M. Robertson, Nature (London) **164**, 915 (1949).
[4] P. Groth, Acta Chem. Scand. **17**, 2419 (1963).
[5] B. S. Cartwright and J. H. Robertson, Chem. Commun. (Cambridge) **1962**, 82 (1966).
[6] A. Kvick, R. K. McMullen, and M. D. Newton, J. Chem. Phys. **76**, 3754 (1982).
[7] D. W. Smith and K. Hedberg, J. Chem. Phys. **25**, 1282 (1956).
[8] B. W. McClelland, G. Gundersen, and K. Hedberg, J. Chem. Phys. **56**, 4541 (1972).
[9] K. B. Borisenko, M. Kolonits, B. Rozsondai, and I. Hargittai, J. Mol. Struct. **413–414**, 121 (1997).
[10] C. A. Coulson and J. Duchesne, Bull. Cl. Sci., Acad. R. Belg. **43**, 522 (1957).
[11] H. A. Bent, Inorg. Chem. **2**, 747 (1963).
[12] L. Pauling, *The Nature of the Chemical Bond*, 2nd ed. (Cornell University Press, Ithaca, NY, 1960), p. 349.
[13] J. M. Howell and J. R. Van Wazer, J. Am. Chem. Soc. **96**, 7902 (1974).
[14] R. Ahlrichs and F. Keil, J. Am. Chem. Soc. **96**, 7615 (1974).

[15] C. W. Bauschlicher, Jr., A. Komornicki, and B. Roos, J. Am. Chem. Soc. **105**, 745 (1983).
[16] A. Stirling, I. Papai, J. Mink, and D. R. Salahub, J. Chem. Phys. **100**, 2910 (1994).
[17] R. Liu and X. Zhou, J. Phys. Chem. **97**, 4413 (1993).
[18] M. L. McKee, J. Am. Chem. Soc. **117**, 1629 (1995).
[19] A. Kovacs, K. B. Borisenko, and G. Pongor, Chem. Phys. Lett. **280**, 451 (1997).
[20] S. S. Wesolowski, J. T. Fermann, T. D. Crawford, and H. F. Schaefer, III, J. Chem. Phys. **106**, 7178 (1997).
[21] M. Kawasaki, K. Kasatani, H. Sato, H. Shinohara, and N. Nishi, Chem. Phys. **78**, 65 (1983).
[22] W. N. Sisk, C. E. Miller, and H. S. Johnston, J. Phys. Chem. **97**, 9916 (1993).
[23] J. Mason, J. Chem. Soc. Dalton Trans. I **1975**, 19.
[24] W. von Niessen, W. Domcke, L. S. Cederbaum, and J. Schirmer, J. Chem. Soc., Faraday Trans. 2 **74**, 1550 (1978).
[25] H. S. Johnston and R. Graham, Can. J. Chem. **52**, 1415 (1974).
[26] T. C. Hall, Jr. and F. E. Blacet, J. Chem. Phys. **20**, 1745 (1952).
[27] A. M. Bass, A. E. Ledford, Jr., and A. H. Laufer, J. Res. Natl. Bur. Stand. **80A**, 143 (1976).
[28] H. H. Holmes and F. Daniels, J. Am. Chem. Soc. **56**, 630 (1934).
[29] G. Inoue, Y. Nakata, Y. Usui, H. Akimoto, and M. Okuda, J. Chem. Phys. **70**, 3689 (1979).
[30] L. J. Butler, D. Krajnovich, Y. T. Lee, G. Ondrey, and R. Bersohn, J. Chem. Phys. **79**, 1708 (1983).
[31] P. Felder, X. Yang, and J. R. Huber, Chem. Phys. Lett. **215**, 221 (1993).
[32] T. L. Myers, N. R. Forde, B. Hu, D. C. Kitchen, and L. J. Butler, J. Chem. Phys. **107**, 5361 (1997).
[33] K. Q. Lao, E. Jensen, P. W. Kash, and L. J. Butler, J. Chem. Phys. **93**, 3958 (1990).
[34] P. C. Ray, M. F. Arendt, and L. J. Butler, J. Chem. Phys. **109**, 5221 (1998).
[35] M. F. Arendt and L. J. Butler, J. Chem. Phys. **109**, 7835 (1998).
[36] M. J. Frisch, G. W. Trucks, H. B. Schlegel *et al.*, GAUSSIAN 94, Revision E.2 (Gaussian, Inc., Pittsburgh, PA), 1995.
[37] C. Dyer and P. J. Hendra, Chem. Phys. Lett. **233**, 461 (1995).
[38] F. Melen and M. Herman, J. Phys. Chem. Ref. Data **21**, 831 (1992).
[39] G. Herzberg, *Molecular Spectra and Molecular Structure*, 2nd ed. (Krieger, Malabar, FL, 1966), Vol. 3, p. 174.
[40] W. S. Struve, *Fundamentals of Molecular Spectroscopy* (Wiley, New York, 1989), pp. 246–247.
[41] K. Q. Lao, M. D. Person, P. Xayariboun, and L. J. Butler, J. Chem. Phys. **92**, 823 (1990).
[42] J. R. Ohlsen and J. Laane, J. Am. Chem. Soc. **100**, 6948 (1978).
[43] C. H. Bibart and G. E. Ewing, J. Chem. Phys. **61**, 1284 (1974).
[44] J. Koput, J. W. G. Seibert, and B. P. Winnewisser, Chem. Phys. Lett. **204**, 183 (1993).
[45] F. Bolduan and H. J. Jodl, Chem. Phys. Lett. **85**, 283 (1982).
[46] J. Danielak, U. Domin, R. Kepa, M. Rytel, and M. Zachwieja, J. Mol. Spectrosc. **181**, 394 (1997).
[47] SPARTAN 5.0, Wavefunction Inc., 18401 Von Karman Ave., Ste. 370, Irvine, CA 92612.
[48] J. B. Foresman, M. Head-Gordon, J. A. Pople, and M. J. Frisch, J. Phys. Chem. **96**, 135 (1992).
[49] H. Katagiri and S. Kato, J. Chem. Phys. **99**, 8805 (1993).
[50] D. Imre, J. L. Kinsey, A. Sinha, and J. Krenos, J. Phys. Chem. **88**, 3956 (1984).
[51] B. R. Johnson, C. Kittrell, P. B. Kelly, and J. L. Kinsey, J. Phys. Chem. **100**, 7743 (1996).
[52] D. L. Phillips and A. B. Myers, J. Phys. Chem. **95**, 7164 (1991).